CHALMERS

Field test of tension piles

-on the long-term behaviour

JORGE YANNIE
CLAES ALÉN

Civil and Environmental Engineering
CHALMERS UNIVERSITY OF TECHNOLOGY
Göteborg, Sweden 2015

TECHNICAL REPORT IN GEOTECHNICAL ENGINEERING

Field test of tension piles

-on the long-term behaviour

JORGE YANNIE
CLAES ALÉN

Civil and Environmental Engineering

CHALMERS UNIVERSITY OF TECHNOLOGY

Göteborg, Sweden 2015

Field test of tension piles
-on the long-term behaviour
JORGE YANNIE
CLAES ALÉN

Technical report 2015:01
ISSN 1652-8549
Civil and Environmental Engineering
Chalmers University of Technology
SE-412 96 Göteborg
Sweden
Telephone: +46 (0)31-772 1000

Cover:
Frame for loading the piles with constant tension loads

Chalmers Reproservice
Göteborg, Sweden 2015

Field test of tension piles
-on the long-term behaviour
Technical report in Geotechnical Engineering
JORGE YANNIE
CLAES ALÉN
Civil and Environmental Engineering
Chalmers University of Technology

Abstract

This report presents the results from a field test carried to study the long-term response of driven tension piles in natural soft clays. The study site was located at Marieholm, Gothenburg. This area is characterized for having deep deposits of natural soft clays, extending up to 100 meters deep. A novel loading rig has been developed for application of constant loads over long periods of time.

Generally, tension piles serve as anchor structures that mobilise the bearing capacity by means of shaft friction. This pile type is less common in Swedish on-shore engineering practice, and only a few cases have been studied where the long-term response has been investigated. Existing research, on offshore piles, indicates that the long-term pile response is governed by the creep behaviour in the natural soft soils (St John et al., 1983; Ramalho Ortigaäo and M. Randolph, 1983). In the present work similar results have been obtained, i.e. the long-term creep behaviour depends on the load magnitude, which in turn governs the displacement magnitude over time. Furthermore, the bearing capacity is limited by the long-term shear strength of the clay (i.e. quasi-static drained shear strength). Finally, the results suggest that creep rupture can be triggered if the pile is loaded close to this long-term failure limit.

Keywords: soft clay, piles, tension load, field test, creep rupture, long-term

Notation

K_0	Coefficient of lateral earth pressure
Q_{ult}	Ultimate state bearing capacity
S_u	Undrained shear strength
α	Total stress factor for shaft capacity
β	Effective stress factor for shaft capacity
μ_i^*	Intrinsic creep parameter
μ_v^*	Deviatoric creep parameter
μ_v^*	Volumetric creep parameter
$\phi^{'}$	Friction angle at the pile-soil interface
ϕ_{cs}	Critical state friction angle
ε_d^c	Deviatoric creep
ε_v^c	Volumetric creep

Contents

1 Introduction

1.0.1 Background

This report presents the results from a field test performed by the Geo-engineering Division at Chalmers University of Technology (CTH) to study the effects occurring over time of displacement piles loaded in tension in natural soft clays (from here onwards called tension piles). This study was part of a PhD research project carried out by Jorge Yannie at CTH in connection with the Västlänken (West link) railway tunnel to be build in Gothenburg, Sweden.

The complexity and size of new on-land infrastructure projects has challenged the current geotechnical design practices. Deeper and wider excavations in soft and sensitive clays posses new challenges for the geotechnical engineers. A current example is the West link railway tunnel project in Gothenburg. Part of the tunnel and some of the stations will be built in very soft clay deposits. Therefore, a good understanding of the soil-structure interaction will help to reduce uncertainties in the design. Recent research in Sweden about excavations in soft clays and long-term term behaviour of the soils in Gothenburg has increased the knowledge and reduced the gaps in this research area (Persson, 2004; Kullingsjö, 2007; M. Olsson, 2010; M. Olsson, 2013). On the other hand, most of the pile research for piles in clays was performed between the 70's and 80's, with a mayor focus on the ultimate limit state of compression loaded piles (Fellenius, 1972; Torstensson, 1973; Bengtsson and Sällfors, 1983) and the foundation settlement as a whole (Jendeby, 1986).

Based on this previous research the ultimate limit state design (ULS) of piles in soft soils is conducted using semi-empirical methods. The most common method for piles in clay is the total stress method (α-method) (C. Olsson and Holm, 1993). This approach has been further calibrated for local conditions, most of those tests being short-term compression loading of driven piles. By experience, it is known that the bearing capacity in short-term is independent of loading direction (C. Olsson and Holm, 1993; Lehane and Jardine, 1994), thus the same design methods are used in tension. However, one issue that remains unclear is the long-term behaviour of pile loaded in tension.

Tension piles are common structures in the offshore industry, where platforms located in deep waters require an anchoring system to sustain buoyancy forces. These piles became very important in the 1980's with the new concept of Tension-Leg platforms (Bradshaw et al., 1984; Jardine and Potts, 1988). During this period, several researchers stated that the soil creep behaviour is the main factor dominating the pile response under long-term sustained tension loads (St John et al., 1983; Ramalho Ortigaäo and M. Randolph, 1983) and should be considered in the design. On the other hand, tension piles are less common in on shore foundations and few cases can be found in the literature. Some example of tension loads for on shore pile foundations are the heave and hydraulic gradients in deep excavations or wind loads for tall buildings (generally not permanent loads).

The Serviceability Limit State is dominant for the long-term behaviour of tension piles (i.e. the soil creep behaviour). The type of creep at the pile shaft is deviatoric or creep under shear

loading. Most of the creep studies focus on volumetric creep, only a few well-documented deviatoric creep investigations can be found (Augustesen, Liingaard, et al., 2004; Liingaard et al., 2004). It is therefore important to investigate the creep behaviour of clays to assist the interpretation of the tension pile response.

1.0.2 Objectives

The research objective is to design and execute a field test for providing qualitative and quantitative insight into the behaviour of piles subjected to long-term constant tension loads in natural soft clays. In order to achieve this, a novel, simple cost effective, compact and robust loading set-up to test piles loaded in tension will be developed with sufficiently constant load application.

1.0.3 Limitations

- The investigation is limited to a short element of a concrete displacement pile of standard cross section, installed by jacking in soft natural clay. The short length of these pile elements do not reflect clearly the progressive failure experienced by long-piles.
- Only monotonic loading after pile installation and set-up will be applied in a stepwise manner until failure is reached.
- Only semi-empirical approaches are used for the interpretation of the results with further processing and calculations in general purpose spreadsheet and engineering software such as MATLAB, Microsoft Excel and MathCAD. Hence, no finite element analysis is done.
- The area was affected by ongoing construction works.

2 On the long-term pile response in clays

This chapter aims to provide some important theoretical aspects of pile foundations. It is by no means a complete summary of all possible aspects, but rather a short description of selected points.

In Sweden, a large body of research has been published the response of piles in natural soft clays. For example, Torstensson (1973) noticed that the ultimate bearing capacity is influenced by the clay rate-dependency. He also showed that the pile material had no significant effect on the shaft capacity. Fellenius (1972) reported results of a major field study to understand the negative friction effect on piles (sometimes called down drag). The results showed that in addition to consolidation the creep settlements in the soil around the pile can generate a significant drag load. Bengtsson and Sällfors (1983) performed several field test to study the ultimate bearing capacity of floating piles in tension and compression. They observed that

the capacity did not vary much owing to load direction and that it increases with time after installation (set-up effects). Furthermore, they noticed a critical load where the creep rate increases sharply, ranging from 75-85% the ultimate bearing capacity (Q_{ult}). In addition, an α=0.9 for uncorrected vane shear tests approximated their tests results well and they corrected their calculation for rate effects. A recent study was done by Pålkommissionen (Hermansson et al., 2015) to compare dynamic pile load tests against static load testing of tension and compression piles. Again the load direction did not show any significant difference in capacity for the static load testing.

Following the results from previous investigations, today practices are based on semi-empirical relations calibrated that are further calibrated for the local conditions. The total stress approach is the common method for design of pile foundations (C. Olsson and Holm, 1993; Eriksson et al., 2004(PK100)). These relations work well in general cases, but are limited to the type of piles, soil and procedures used to derive them.

2.1 Installation, set-up and loading of piles in clay

The installation of driven piles in clays generates distortion of the soil surrounding the pile element. This issue is a topic of research by itself and has been investigated by several researchers (M. F. Randolph et al., 1979; Baligh, 1985; Whittle, 1987; Sagaseta et al., 1997; Basu et al., 2013; among many others). It is known that the driving displacement piles in clay creates large volume displacement of the soil by the pile element penetration. This remoulds the soil under the pile toe and around the shaft, and increases the total lateral stresses in the soil (see Figure 2.1) directly after installation.

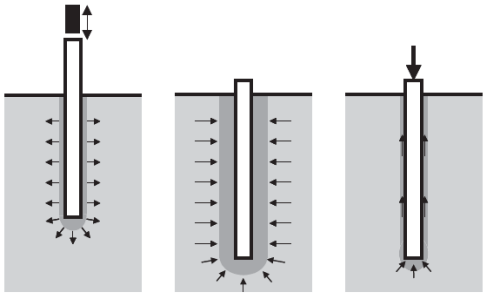

Figure 2.1: *Installation, equalization and loading of a driven pile (adopted from M. Randolph, 2003)*

Following the installation stage, the regain in bearing capacity related to the equalization of the excess pore water pressures and ageing processes is called the *set-up* time. During this time, the soil is in a transition of increasing effective stresses and changes in its properties, e.g. change in void ratio. It can also experiences effects as thixotropy and structuration (Augustesen, Andersen, et al., 2006). In contractive clays, such as those in Gothenburg, this increase in effective stress generally is combined with a decrease in total stress.

The above processes create a new equilibrium state before loading, where the soil around the pile experiences new stress conditions and properties. An example of the expected stress

conditions after set-up is given in Figure 2.2, using the constitutive model MIT-E3 and the cavity expansion method (CEM) and strain path method (SPM). In this example, it is assumed that the SPM gives a better prediction due to the more complex strain paths and one can see that $\sigma_v^{'}$ reduces with 60% near the shaft, with the effective stresses at the shaft close to isotropic conditions. However, there can be limitations in the model and finite element scheme used to make this estimation. Consequently, it is hard to explain with accuracy and details the exact conditions before loading owing to the complexity of the problem. Therefore empirical methods dominate in pile calculations, since they implicitly incorporate these effects.

The axial load is transferred to the soil by shaft friction, see Figure 2.3, and the loading conditions are similar to those in the direct simple shear test (Lehane and Jardine, 1994). The main deformations are from shearing of the soil, which can lead to volume changes depending on the soil behaviour (contractant or dilatant). The additional shear stress create a rotation of the principal stresses and volume changes will either decrease or increase the radial stresses.

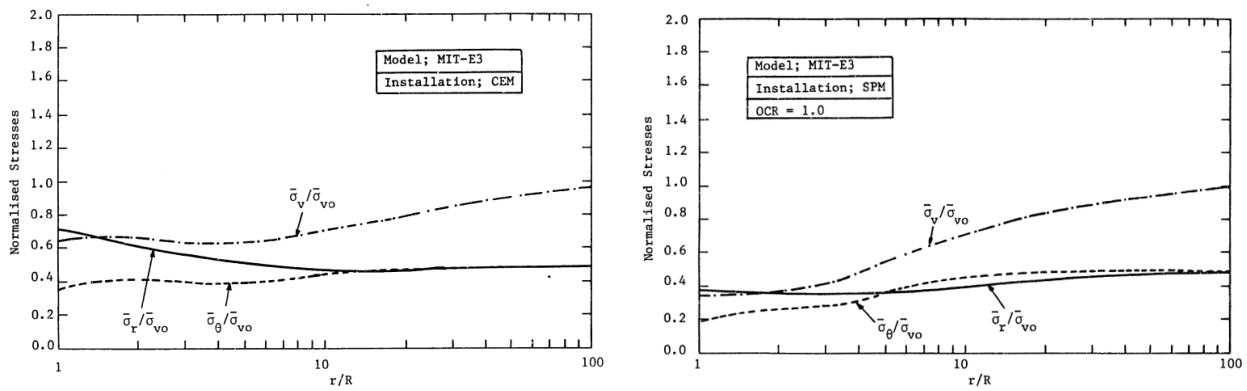

(a) (b)

Figure 2.2: *Numerical model results of effective stresses after installation and set-up for Boston blue clay with OCR=1 (adopted from Whittle, 1987)*

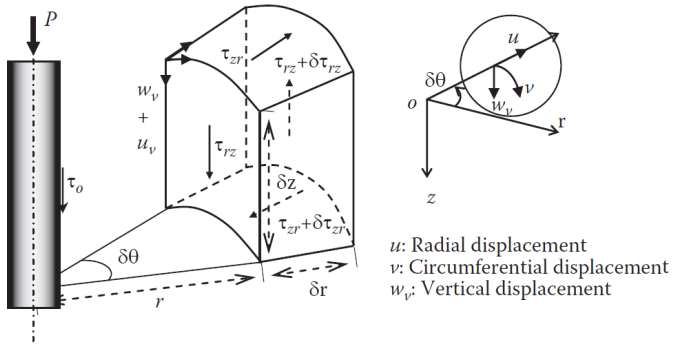

Figure 2.3: *Stresses and displacements at the shaft by axial loading of the pile (adopted from Guo, 2012)*

2.2 Ultimate limit state (ULS)

In Scandinavia, the short-term bearing capacity (ultimate limit state, ULS) is typically calculated using empirical or semi-empirical methods (Karlsrud, 2014). Two of the most common approaches used are the α and β methods (total and effective stress respectively) shown in equations (2.2) and (2.2).

$$Q_{ult} = \alpha \cdot S_u \cdot A_{shaft} \tag{2.1}$$

$$\begin{aligned} Q_{ult} &= \beta \cdot \sigma_{v0}^{'} \cdot A_{shaft} \\ \beta &= K_0 \cdot \tan(\phi_{int}^{'}) \end{aligned} \tag{2.2}$$

In Sweden, the α method is typically used for ULS design of pile foundations. This approach is based on the undrained shear strength of the clay and calculation of the ultimate failure load (Q_{ult}) is done in combination with safety factors. The latter account for other variables, as for example the long-term response of the pile. Typical characteristic values for the α parameter range from 0.9 to 0.95 for soft Gothenburg clays, for S_u values obtained from uncorrected vane shear tests. Note that S_u is affected by the rate of rotation used in standard vane tests and the quality in the procedure. As a consequence some error is inherit in the calculations.

2.3 Serviceability limit state (SLS)

The serviceability limit state refers to the long-term behaviour of the piles under working loads. Design methods in Sweden do not explicitly account for long-term creep deformations. One case where creep is considered is in the design of creep-piles foundations (a type of pile-raft foundation). In this foundations the piles are loaded to fail by creep, the creep load being in the range of $(0.6 - 0.8)Q_{ult}$, allowing for whole foundation to settle with a more uniform and better use of the capacity (Hansbo, 1984; Jendeby, 1986). Otherwise, creep of piles under sustained load have not been fully investigated in a more general framework.

In this report the focus is given to the creep process resulting from deviatoric (shear) loading of clays.

2.3.1 Deviatoric creep

According to the definition of creep in soils, pure creep processes only occur with constant effective stresses, i.e. drained creep (Augustesen, Liingaard, et al., 2004). During undrained conditions, the effective stresses decrease with the build-up of creep induced pore water pressure, therefore the observed creep cannot be called “pure” creep. For the pile case, the long-term

response is considered to be under drained conditions; thus fulfilling the condition for pure creep.

The measured displacement at the pile head can be divided into three different components. The first and second contribution are from the soil instantaneous elastic response and from the consolidation triggered by any shear-induced excess pore water pressure. The third arises from the deviatoric creep at the pile shaft. It is this creep deformation that governs the long-term response of the piles (St John et al., 1983; Ramalho Ortigaäo and M. Randolph, 1983). This creep will develop around the shaft in the area of influence of the shear load.

Deviatoric creep has been studied in laboratory conditions by several authors by means of, drained and undrained, triaxial and direct simple shear tests (J. Mitchell and Soga, 2005; Tian et al., 1994; Tavenas et al., 1978). These tests can develop the three phases of creep, namely (1) primary or fading, (2) secondary or stationary and (3) tertiary or accelerating creep, as shown in Figure 2.4; while 1D oedemoter tests only can exhibit the primary phase. Secondary and tertiary creep ultimately will lead to creep rupture (i.e. failure).

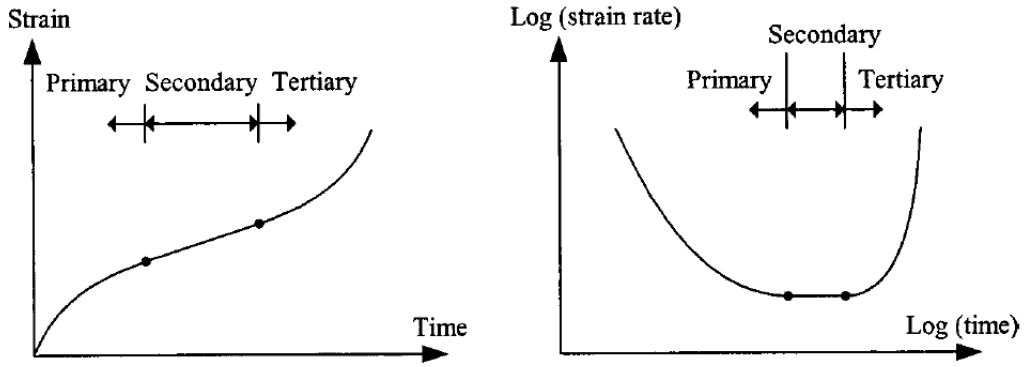

Figure 2.4: *Creep phases in triaxial conditions with constant total stresses (adopted from Augustesen, Liingaard, et al., 2004)*

2.3.2 Creep rupture

Creep rupture is defined as the failure following the tertiary creep phase due to strength reduction in the soil. Several effects caused by creep can contribute to the loss of strength in clays (J. Mitchell and Soga, 2005), as for example:

- It will contribute to de-structuration processes.
- It can cause change in effective stresses by relaxation if there are kinematic constrains.
- It can generate excess pore water pressure and therefore a reduction in effective stress. For example, if high creep rates develop, the dissipation of excess pore water pressure might be slower than the rate of increase of Δu, and therefore a decrease in $\sigma^{'}$.
- It can change the water content, and thus change the strength. For example, at the pile shaft this can reduce the rate of dissipation of excess pore water pressure from the critical

zone due to the reduction of permeability (Δu reduces σ').

The main difference for creep rupture in deviatoric creep tests arises in when drained and undrained tests are compared. Campanella and Vaid (1972) did a study on natural clay from Haney, British Columbia (Canada) and showed that after a certain deviatoric stress, undrained tests experienced creep rupture at approximately the same accumulated strain. The tests were loaded at various stress levels, giving different creep rates and therefore diverse times to failure. On the other hand, studies done by Tavenas et al. (1978) and Tian et al. (1994) revealed that drained deviatoric creep tests behave mainly under the primary creep phase, and only experience creep rupture if loaded close to the limit state surface (stress-level dependency). Therefore, one can believe that the long-term response is governed by a pure frictional law in quasi-static drained conditions, where primary creep will occur within a limiting failure surface (see Figure 2.5).

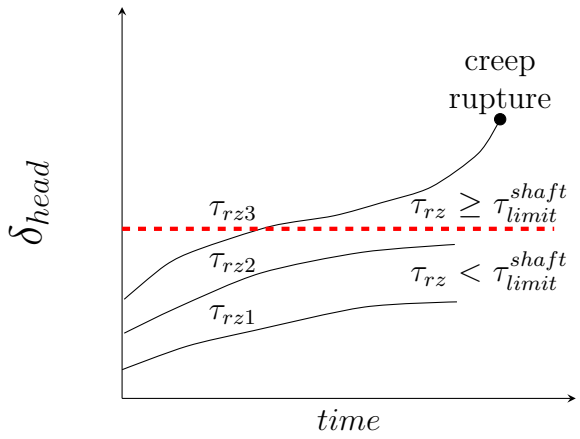

Figure 2.5: *Illustration showing a limit shear strength where below it creep rupture will not develop.*

2.4 Creep curves, models and extrapolation

Modelling of creep can be done in several ways, for example by empirical models, rheological models or general stress-strain-time constitutive laws. A good summary of the different approaches to model creep is given by (Liingaard et al 2004) and some details can be found in the PLAXIS manual (www.plaxis.nl) and J. Mitchell and Soga (2005). The most common theoretical approach is to use an empirical logarithmic law as given in equation (2.3) (Bjerrum and Janbu ideas, see PLAXIS manual). This type of model is based on 1D compression and can only predict primary creep (drained conditions), with the creep strains having a linear relation with the logarithm of time (note that ε = logarithmic or Hencky strains). Furthermore, this model predicts a unique relation between the accumulated creep deformations and time (isotachs).

$$\varepsilon_v^c = \mu_v^* \cdot \ln\left(\frac{t_{ref} + t}{t_{ref}}\right) \tag{2.3}$$

Generalization of this empirical model to 3D space make it possible to determine the deviatoric creep strains by means of a flow rule (for example see Sivasithamparam et al., 2015). However, it is assumed that for the deviatoric creep at the pile shaft, the same 1D volumetric creep equation can be used by adopting a deviatoric creep parameter, as shown in equation (2.4). The μ_d^* was obtained from the field measurements, but it might be possible to obtained it by mean of triaxial creep test by measuring the deviatoric creep.

$$\varepsilon_d^c = \mu_d^* \cdot \ln\left(\frac{t_{ref} + t}{t_{ref}}\right) \tag{2.4}$$

The creep parameter in equation (2.3) and (2.4) is the slope of the linear end-part of the measurement curve in a ε-ln(t) plot. This parameter is not constant and it is a function of stress and strains (i.e. void ratio), $f(\sigma, e)$ (Jostad and Yannie, 2015). For a fully remoulded soil, this parameter is nearly constant and is called the intrinsic creep parameter μ_i^*. For practical calculations, μ_v^* is selected based on the working stress range. Because of the remoulding process caused by pile installation, one will expect this parameter to be close to the intrinsic value and therefore, the stress dependency might not be that dominant as for undisturbed clays.

The time reference in the above equations is usually taken as the time after primary consolidation. For an incremental loading oedometer test (IL), this time is around a couple of hours within the 24 hours of each step, but for practical purposes it is assumed as 1 day. Therefore, the IL curve is called the 1 day curve. For the pile case, each load step was held for a different amount of time, making it difficult to assume a reference time.

Not all clays exhibit this type of linear behaviour with the logarithm of time and non-linearity can be observed (J. Mitchell and Soga, 2005). For example, if the applied load is close to the apparent pre-consolidation pressure, the soil might experience larger strains caused by de-structuration. The latter will change the soil behavior (new structure) and therefore non-linearity can emerge. Furthermore, after a long creep period the deformation rate will become so slow that processes as chemical bonding could take over creep and the linear relation is again not valid. If one incorporate these variations into the model, the non-linear behaviour can be captured (Liingaard et al., 2004; Jostad and Yannie, 2015) but for practical purposes, equations 2.3 and 2.4 give a good approximation.

3 Materials and Methodology

The following section describes the system developed to study tension loaded piles in the field. A description of the test site and soil characterization, types of piles and materials, mechanical parts, instrumentations and methodologies used are given in a corresponding subsection.

3.1 Test site

The criterion for selection of the test site was to have a soft soil of similar characteristics as those expected in the construction path of the Västlänken project. The selected site was located within the PEAB working area for the Marieholmsförbindelsen project at Marieholm, Göteborg (see Figure 3.1 coordinates 6402173, 321345; SWEREF99 system). The location is part of the extensive Göta river sedimentation basin. This clay deposit extend all the way to central station, where Västlänken will start and where most of the tension piles are expected.

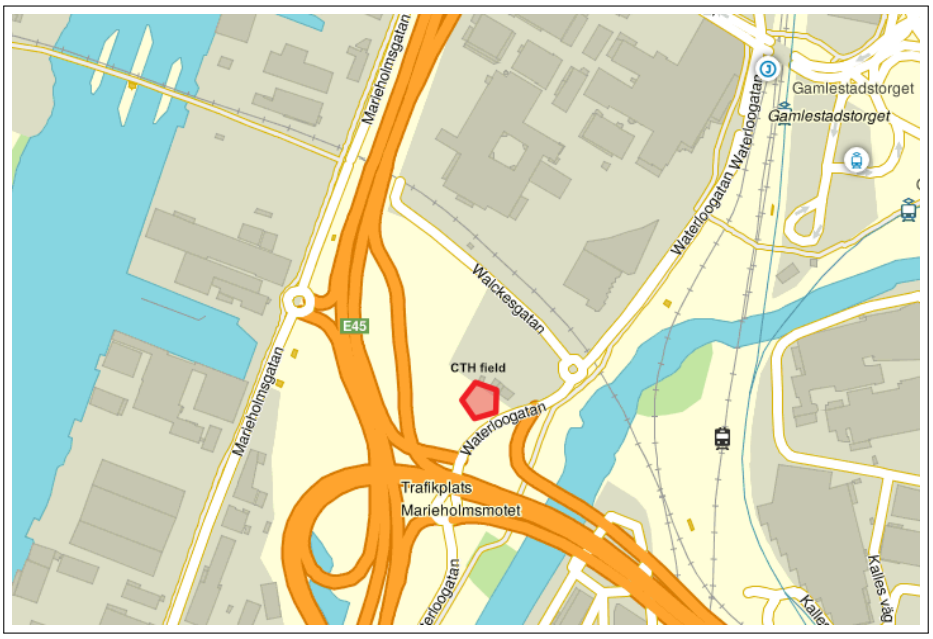

Figure 3.1: *Marieholm area. The red pentagon represents the test site.*

The site arrangement and soil investigations are shown in 3.2. This area has been previously filled up and during the recent years it has been an active construction site for projects like the Partihallsförbindelsen and Marieholmsförbindelsen. The first 1.9 to 2 meters of soil is a mix of filling material (gravel, sand, silt) and clay, followed by a thin stiff clay layer of approximately 0.3 meter. Thereafter, deep deposits of rather homogeneous post-glacial and glacial clays can be found up to 100 meters deep. The deposit is rather young in geological time (10,000 years) and it experiences on-going settlements. The latter could be an additional variable affecting the pile response, however it is not yet clear. One assumption is that the low creep rate will not affect the test within the time frame of the field test.

3.1.1 Soil characterization

In-situ and laboratory tests were performed to characterize the soil in the area. In the field, a cone penetration test (CPT), a shear vane test (Vt) and extraction of samples by mean of a piston sampler were carried out. Table 3.1 shows the number of laboratory tests done, and Figure 3.3a and 5.1 show some of the results (the id code for these tests is CTH TP1).

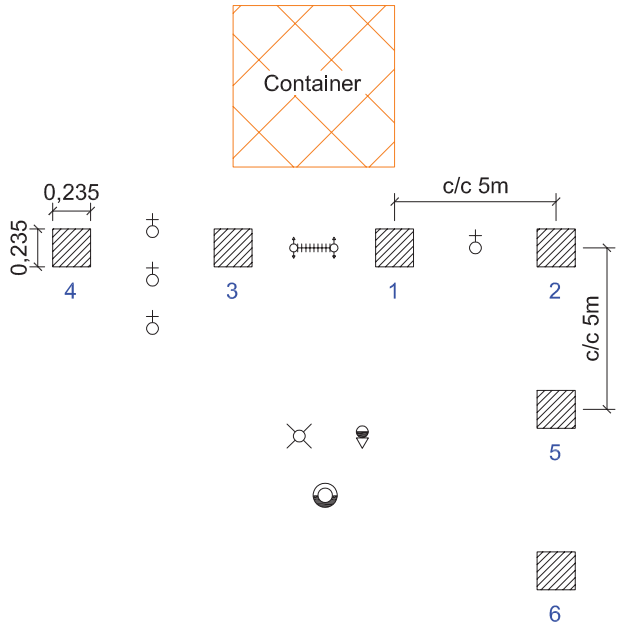

Figure 3.2: *Site arrangement, soil investigations and instrumentations.*

Table 3.1: Laboratory tests from the test site soil

Depth [m]	IL	CRS	DSS	CAUC
13	1	-	-	1
14	1	1	1	1
16	1	1	1	1
18	-	1 (1)*	1	-

IL: stepwise oedometer, CRS: constant rate of strain oedometer, DSS: direct simple shear, CAUC: anisotropically consolidated undrained triaxial compression.
* Numbers in parentheses are disturbed tests.

The soil in the area is very homogeneous. The clay is very soft, sensitive and lightly overconsolidated; with the water content almost equal to the liquid limit at all depths. A critical state friction angle ϕ_{cs} between 38-41 degrees was found in the triaxial tests (in $p^{'} - q$ plot).

The groundwater level was found to be approximately 0.30m below the ground surface. In order to monitor the pore water pressure during the test, four BAT piezometers where installed at depth of 11, 15 (two units) and 19 meters. One of the 15m unit stopped working after 1 month. Measurement of the average pore water pressures are showed in Figure 3.3b, together with previous nearby measurements. The measurement showed that there is some excess pore water pressure below ≈5 meters deep.

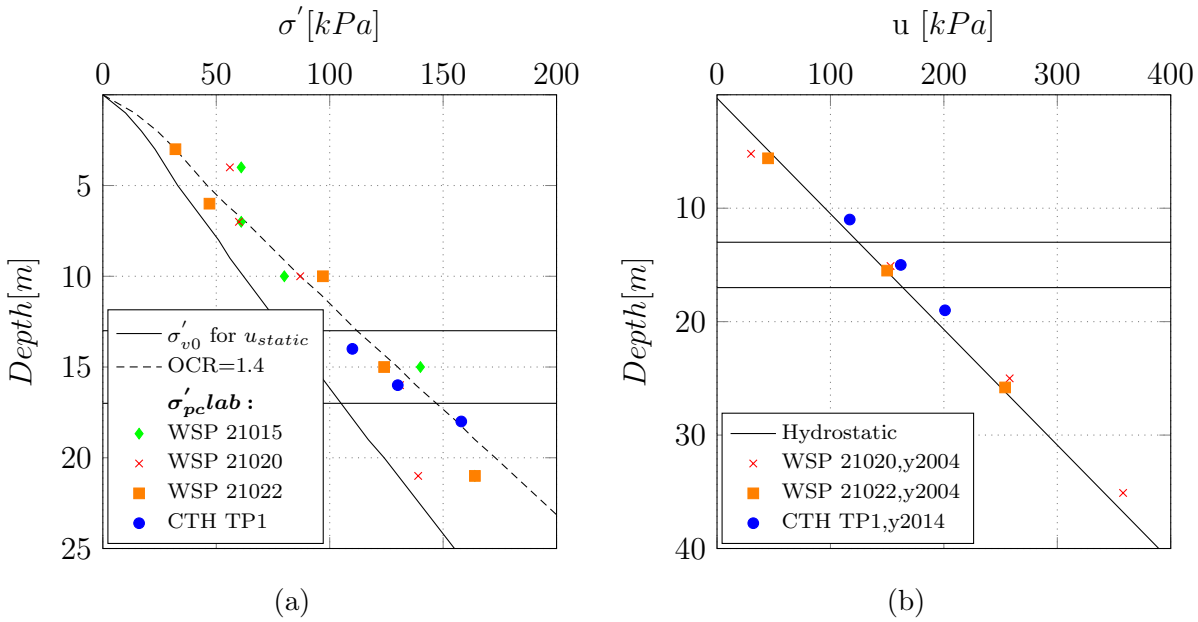

Figure 3.3: *(a) Pre-consolidation pressure, (b) Average u in the area, year 2004 and 2014.*

3.2 Pile elements

A total of 6 pre-cast reinforced concrete piles (C5060/B500CT) of 4.20 meters length and cross section of 235x235mm (4m concrete + 0.20m steel; equal to 1/3 of standard pile element) were used in the experiment (see Figure 3.4). The size of the pile made them behave as nearly rigid bodies, with relatively uniform displacement along the complete pile-soil interface. These short piles in combination with the homogeneous clay in the area, facilitated the interpretation of the results. The weight of one pile together with the pulling rod was approximately 6.45 kN.

A GWS-ϕ=32mm steel rod was used to pull the piles with tension loads. The rod went inside a steel pipe cast in the concrete, all the way to the toe, in order to transfer the load from the bottom and up, creating a compression stresses in the concrete. This was done to avoid any tension cracks and thus preserve the properties of the pile as a continuum. The piles might had experienced some loading eccentricity due to the long pulling rod and the possible initial inclination from the installation.

A steel pile (open pipe) of 220 mm in diameter was used to guide the concrete piles to the desired depth. This pipe served as a fixed point and as a casing, providing a hole for the cables, tell-tales and the pulling rod (see Figure 3.5).

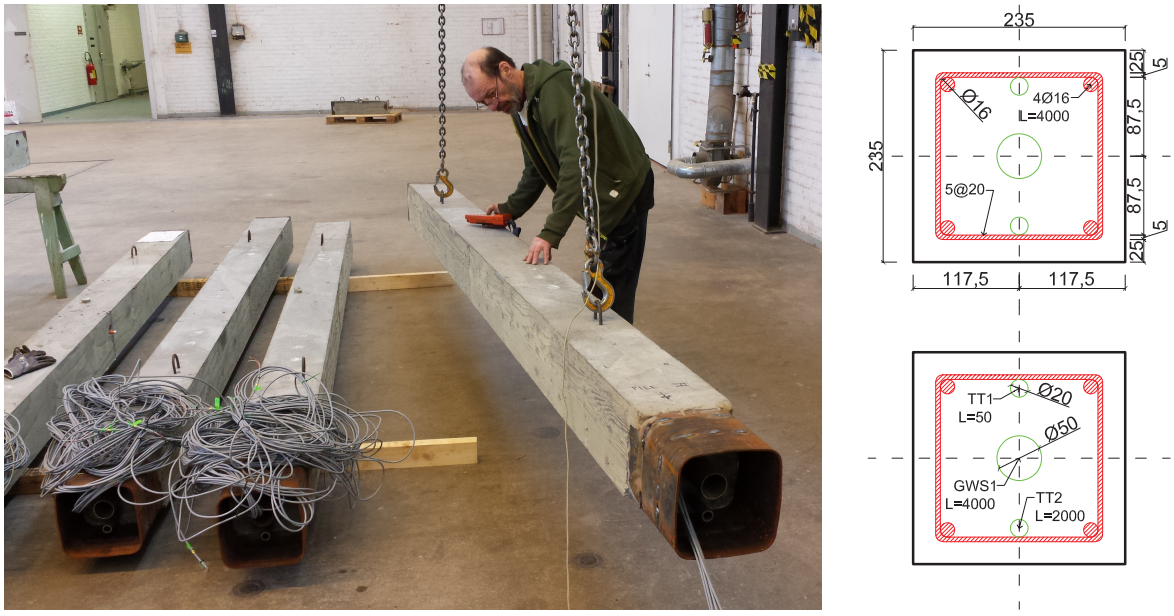

(a) *Concrete+steel fit for over pile* (b) *Cross-section (mm)*

Figure 3.4: *Pile elements.*

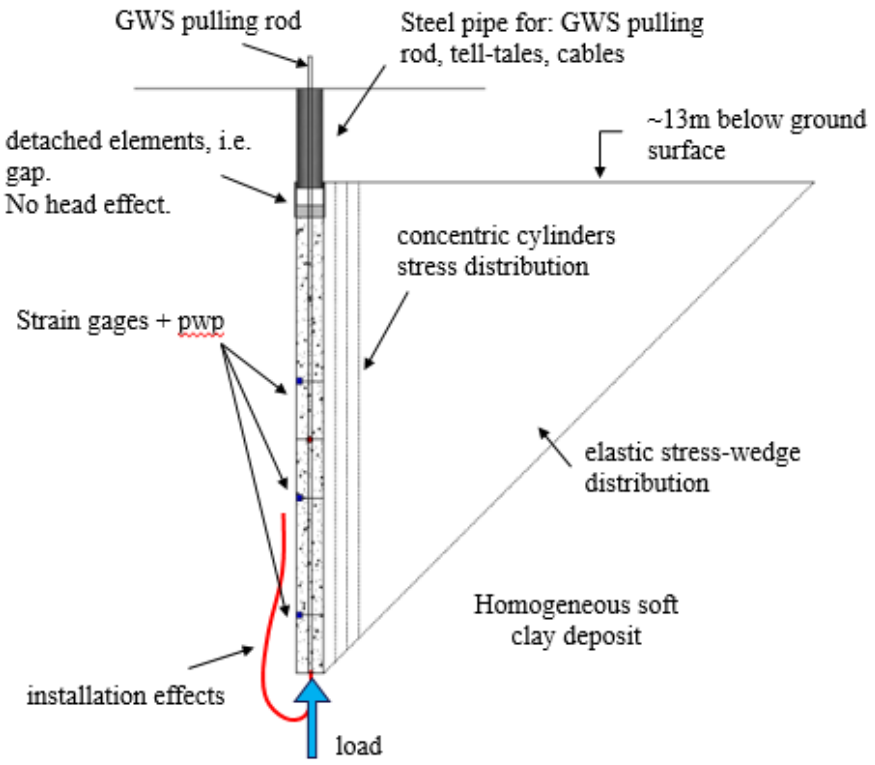

Figure 3.5: *Sketch of the steel guiding pile and concrete pile. Note that the concrete pile is 13m below the ground surface.*

3.3 Instrumentation

The piles were instrumented with ring load cells, strain gages, pore water pressure transducers, tell-tales and linear potentiometers (LP). All instruments were connected to a National Instrument Data Aquisition system model NI-cDAQ9178 equipped with 2 NI9219 and 2 NI9237 channel modules. The instrumentation per pile are listed in Table 3.2. These were calibrated before the start of the test to check their stability and to zero set the measurements.

To measure the internal strains in the pile, strain gages model XY11-6/350 from HBM were glued on sister rebars which were tied up to the main rebars (see Figure 3.6). At each level two sister bars were attached, opposite to each other. This was done in order to have redundancy in the system. The gages were configure as half-bridge, with one gage in the axial direction and the other orthogonal to it to compensate for Poisson's ratio effect and temperature. A model pile of 1 meter long was used to evaluated the strain gages performance. The test was performed at the concrete laboratory of the SP Technical Research Institute, 156 days after the casting of the pile. The results are shown for a loading-unloading-reloading cycle up to 200 kN (see Figure 3.6). The pile deformed around ≈100 me or 0.1 mm and non-linearities were found in the elastic modulus of the reinforced concrete in a range of E=27-33 GPa. Further loading-unloading cycles up to 1000 kN showed a degradation in the modulus and more non-linearities.

Table 3.2: Instrumentation of all piles

Pile	SG	PWP	TT	LP
1	3	2	2	1*
2	3	1	2	1**
3	3	2	2	1*
4	3	1	2	1**
5	3	-	2	-
6	3	-	-	-

* Fixed at aluminium beam.
** Fixed at steel guiding pile.

Four piles were instrumented with pore pressure transducers model PT9544 from IFM at the pile-soil interface. These were installed inside a small canister fixed at the pile shaft. Two piles had one transducer in the mid length and the other two had one on the mid and bottom of the pile.

The displacement of the pile head was monitored using the LPs and tell-tales. The LPs were placed on the top plate that connected the pulling rod with the H-beams. At this measuring point, an additional elastic displacement component from the pulling rod was indirectly incorporated in the measurements. This was corrected in the results. The tell-tales were steel pipes going from the ground level all the way to the pile head and mid section. The latter were measured using mechanical dials, which were fixed at the steel guiding piles.

The fixed points, used for measuring the relative displacement between the pile-soil interface

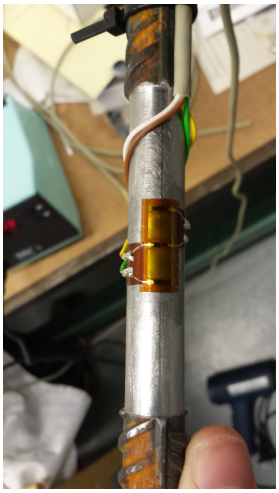

(a)

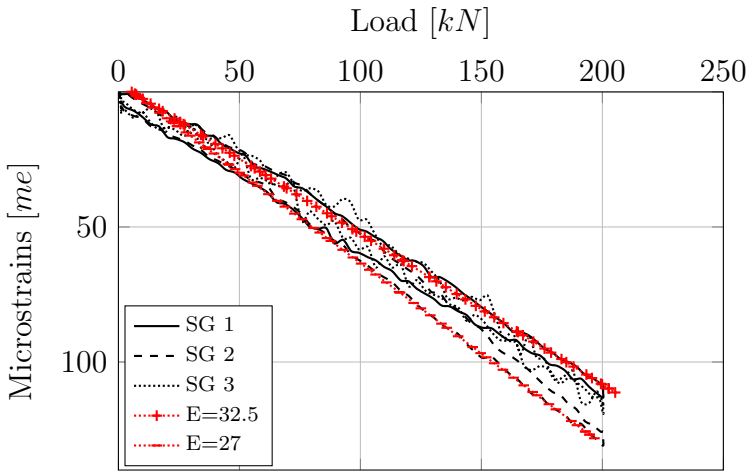

(b) *Three types SG at the mid section of the pile*

Figure 3.6: *(a) Strain gages glued to sister bars (b) Strain gage measurements from a loading-unloading cycle of 1 meter model pile.*

were the steel guiding piles or an aluminium beam going over the loading frame, resting on two supports grounded at ground level. Levelling was done to control the fix points and this had an accuracy of ± 1 mm. Therefore some uncertainty is inherent in the measurements.

3.4 Loading frame

Loading of piles is commonly done by use of hydraulic jacks or kentledge blocks (dead weight). For the case of long-term testing, the former required complex hydraulic control systems while the latter requires large structural elements and a lot of space, material and work force. To overcome these problems, the loading frame was developed based on the spring theory, with a system that stored potential energy. The spring had to preserve most of the energy with any small change in displacements at the pile head. To achieve this, pneumatic lifting bags were used. These bags behaved as non-linear springs and their stiffness is function of the contact area between the reaction points.

The bag used was the TLB32 from Trelleborg, with a lifting capacity up to 32 tons. Two bags were used per pile and they were placed between two plywood sheets on top of the log-floor and underneath the HEB260 steel beams. The air pressure was regulated using solenoid valves connected to the measuring computer or was regulated manually from time to time. The bags and an analytical model of the load-displacement behaviour is presented in Figure 3.7. The load is dependent on the contact area, i.e. the less area the lower the load.

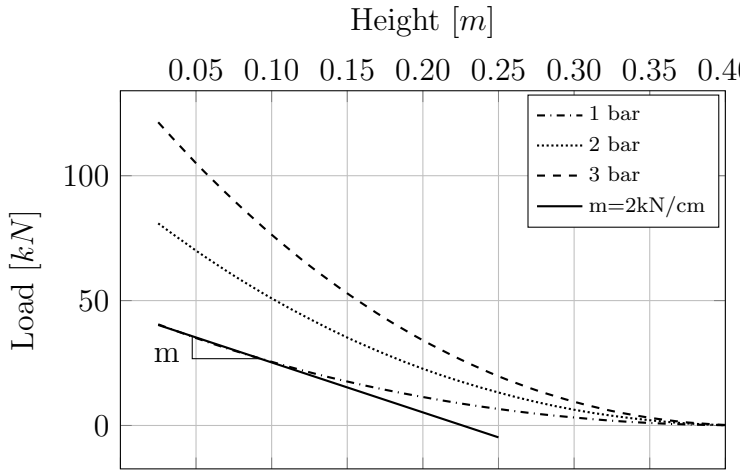

(a) *Analytical model for pressure in bags*

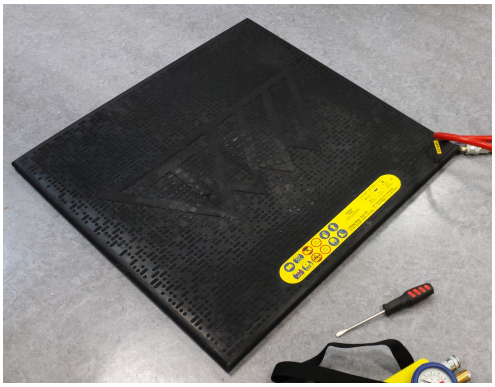

(b) *TLB 32ton bags*

Figure 3.7: *(a) Loading frame (b) Lifting bags*

3.5 Test protocol

Some sections of the Västlänken tunnel will be built mainly on top of glacial clay, with most of the post-glacial clay being excavated (10-20 meters deep excavations). Characterization of the Marieholm soil deposit showed that the post-glacial clay extend up to ≈10 meters below the surface. Therefore, the model piles were installed 13 meters deep from the ground level. Steel piles were used to guide the concrete model piles to the desired depth. The dimensions of these guiding piles were ϕ=220mm and t=15mm.

A total of 6 piles were installed by jacking (pushing with ram) the piles through the clay with a pile-driving rig Junttan PM23lc with a ram weight of 4 tons. A hole was created through the dry crust and filling material with help of a 2 meter long steel closed-pipe. This was done to clear any material from the filling that could stand on the way and to reduce the installation effect on the surface level. After the piles were installed, a fill layer of 0.30-0.40 m was laid on the ground. On top of the filling a log-floor was used to place the lifting bags and to redistribute the reaction loads on the ground.

Short-term tests
In Sweden there is no specific standard for testing piles with tension loads. The pile commission report number 59 for static load testing (Sandegren et al., 1980) mainly refers to piles loaded in compression. Looking at the international literature, it seems that there is also a lack of information for these type of piles. For example, the ISO is currently working to develop a specific standard for tension loaded piles, under the TC182 committee, subcommittee SC1, project 224777. In that respect, it was decided to follow the Swedish guidelines even for tension loads.

An estimate of the ultimate shaft bearing capacity (Q_{ult}) prior to loading was calculated using the α method, with an average Su=30kPa and α=0.9. This resulted in a load of Q_{ult}^{calc} equal to 107kN. It was decided to start loading the piles from a first step of 20-50% of Q_{ult}^{calc} and with

Table 3.3: Short-term pile tests

Pile#	Test	Note	Set-up (days)
5	ST5A	After set-up	207
6	ST6A	After set-up	186
	ST6B	After ST6A+set-up	206

stepwise load steps of 10-15%, as shown in Figure 3.8.

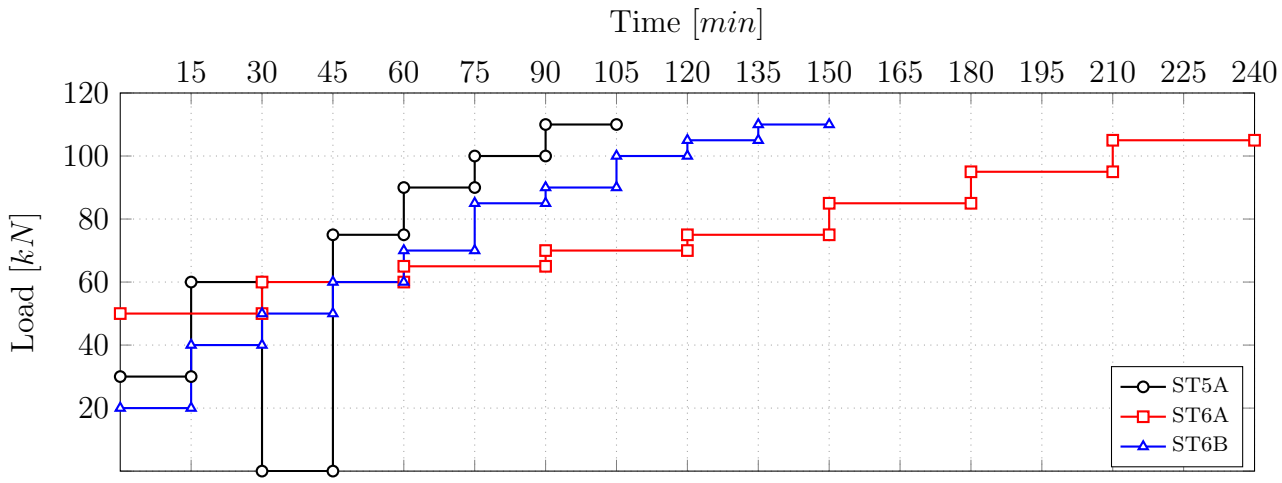

Figure 3.8: *Protocol for short-term tests*

Long-term tests

The long-term loading of the piles was done by stepwise load increments. All piles were pre-loaded with 8-10 kN in order to remove the slack in all the joints of the loading frame and left for one day to stabilize. After that, they were loaded to different load levels given in Table **??**. The hold time for each level was according to two criterias,

- the displacement rate was lower than 0.10mm/60min, or
- until the displacement-time curve showed a tendency to reach an asymptote (in the linear scale).

After having a better understanding of the long-term behaviour from Pile 1 to 4, a new test was done to overcome the encountered challenges. The test was done using Pile 5, which rested for 184 days after been failed in the short-term (ST5A). The load was kept constant with time with solenoid valves controlled by the computer and the displacement measurements were performed directly on the tell-tales. Each load step was increased as soon as the creep rate exhibit a hyperbolic-type of curve tending to an asymptote.

4 Results

This section presents the results and interpretation of the short-term and long-term testing of all piles in the test site.

4.1 Ultimate limit state (ULS)

Short-term tests were carried out to study the bearing capacity in tension after the pile set-up period. The test were done using the quick maintained load method (QML) suggested by the Swedish pile testing guideline. The results show a failure load around Q_{ult}^{unc}=105-110kN and a creep load Q_{creep}^{unc} ≈75kN. These loads needed to be corrected for the pile and GWS rod weight, which was approximately 6.45kN. After correction, one value was selected as the reference Q_{ult}^{ref}, equal to 100kN and the Q_{creep}^{ref} as 70kN.

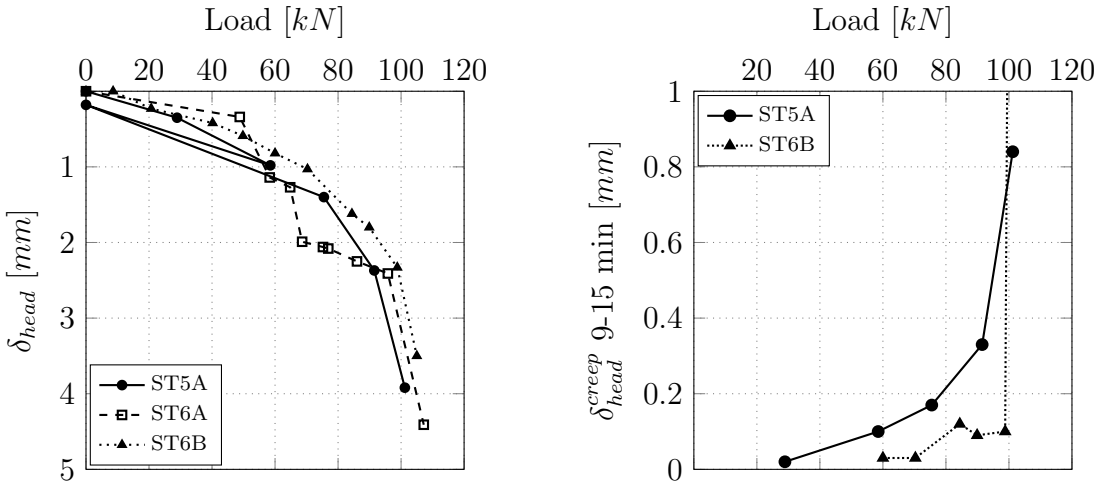

(a) *Load-displacement curves*

(b) *Accumulated creep displacement of last 6 min for each load step*

Figure 4.1: *Short-term results.*

4.1.1 Interpretation of results and back-calculation

Displacement measurements were done at (i) the top plate where the load cell seated and where the GWS pulling rod and the H-beams from the loading frame connected, and (ii) at the head of the tell-tales. It was recognize that the top plate measurement had an inherent elastic displacement component from the pulling rod. In addition, an unforeseen component raised from the plate tilting as the frame slanted because the beams sat on top of two rollers and were not fixed in the out-of-plane direction. Consequently, tell-tales measurements are considered as the true value and all other measurement are corrected against them. The difference in magnitude between the middle and top tell-tale was in a range of 0.30-0.60mm. This difference

is considered too large, since it will be equivalent to a change in load from the middle to the top of the pile equal to 500kN. Hence, the latter is clearly an accuracy problem in the measurements. The average of the tell-tales is presented herein.

(a) *LP at top plate* (b) *LP at tell-tales*

Figure 4.2: *Arrangement of LPs for long-term test of Pile 5.*

In some cases, each time a load step was added the loading frame tilted slightly. After that, the tilting remained fairly constant during the long term deformation. Loading and unloading cycles were done to verify that the tilting that occurred by loading was recovered by unloading. This was done to find an "pseudo-elastic" modulus of the system in order to correct the measurement for this additional displacement component. The latter approach gave an approximation of the real displacement, but there is still some inherent uncertainties in the results from any measurement at the top plate.

The first test (ST6A) with Pile 6 showed an ultimate bearing capacity of Q_{ult}^{corr}=100.8 kN. The displacement measurements were very much blurred by the tilting effect described before. It was therefore decided to do a second test to validate the obtained ultimate bearing capacity and to measure properly the displacements. The second test (ST5A) with Pile 5 resulted in an ultimate bearing capacity of Q_{ult}^{corr}=105.5 kN, which is in close agreement with Pile 6. For this test, the average displacement at failure was about ≈4 mm, which correspond to 1.3% of the pile equivalent diameter(D_{eq}=299.2 mm). In addition, an unloading stage was done at 60 kN, showing that most of the accumulated displacement up to that load were elastic. A third test, experiment ST6B, was done using the pre-failed Pile 6 after a second set-up period. For this case, the frame was fixed to avoid the tilting effect in the out-of–plane direction. The obtained ultimate bearing capacity was Q_{ult}^{corr}=98.5 kN with a failure displacement of ≈3.5 mm. This is in very good agreement with previous results even after pre-failing the pile. The recover in bearing capacity can be attributed to the set-up period after the first failure.

From the experiments ST5A and ST6B the creep load was evaluated following the guidelines of the Swedish pile testing. Both test showed a creep load of approximately 70-80% of the ultimate bearing capacity. Test ST6B showed less accumulated creep for each stage as compared with ST5A. A possible reason is that the pre-shearing and subsequent consolidation reduced the void ratio and the creep effects (the pile behaved stiffer).

Back calculation of Q_{ult}^{ref}=100kN using the total stress approach with the uncorrected vane shear strength resulted in a α value of 0.9 for a Q_{ult}=103.8 kN. In addition, using the effective

stress approach with a friction angle of 30 degrees and a K_0^{shaft} of 0.55, the resulting Q_{ult}=105.2 kN. Both approaches gave very good approximation for the tested piles.

4.2 Serviciability limit state (SLS)

The long-term test was carried out using four piles (Pile 1 to 4). The piles were loaded at the same time with different Q/Q_{ult} ratios. The loads were not constantly regulated, but were adjusted every certain time as needed (keeping the maximum variation within 10% of the actual load Q).The variation in loads was caused by temperature effects and pile displacement.

An additional test was done using the pre-failed Pile 5 in order to compare constant loading against non-constant. The load was constantly regulated by a computer and a pair of solenoid vales. The general observed behaviour was similar to that of having a changing load within certain limits. For this pile, a stiffer response was observed (as in ST6B), with less creep displacements.

The measured pile head displacements over time were also affected by temperature effects do to season changes. In addition, tilting of the frame and the vibrations from the construction site created additional scatter in the measurements. These are described below:

- **Temperature effects**
  The piles were loaded in November 17, 2014 (after a set-up time of 217 days). It was the beginning of the winter season and the temperature fluctuations started to become more noticeable in the upcoming months. This variation affected significantly the experiment; on one hand by changing the air pressure in the bags (i.e. the load) and on the other by creating fluctuations due to thermal expansion of the steel in the frame and rod; which could be measured by the LPs.

- **Tilting**
  For Pile 1 to 4 the LPs were located at the top plate which connected the pulling rod and the ring load cell. At this point the measurement needed to be corrected for the elastic deformation of the GWS rod. However, after correction for the latter, the measurements did not match the magnitude of the mechanical dials at the tell-tales. It was found that the error derived from an additional displacement component caused by tilting of the top plate.

- **Construction site effects**
  Extreme vibrations from heavy-loaded trucks and pile driving created some jumps in the data.

The latter factors generated uncertainty in the data. Since four piles were available (redundancy in the test), the uncertainty in the system could be analysed to some extend.

4.2.1 Interpretation of results

The pure creep definition is based on constant effective stress, as mentioned in section 2.3. However, the piles loads were not held constant during the complete testing period, but were kept within ±5-10% of the load of each step, and therefore the above creep definition can not be applied here (with exception of Pile 5 which was relative constant compared to the other piles). The absolute trend correspond to an unloading of the pile with time. This unload happened very slowly, therefore it is assumed that drained conditions prevailed at all time and thus all measured upward deformations can be attributed to creep. As a consequence, the unloading accelerated the reduction of the creep rate.

Using the isotach framework (see section 2.4) and assuming it is valid for the deviatoric creep at the pile shaft, one can explain the above described situation as illustrated in Figure 4.3. For a load step, the unloading effect will reduce the creep rate and the total deformation for a certain time will be smaller (path A to C) compared to a constant effective stress for the same time (path A to B).

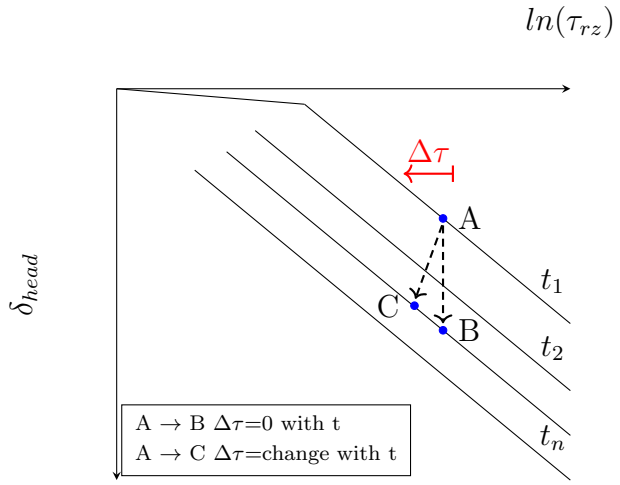

Figure 4.3: *Concept of isotach and unloading of the pile.*

All piles failed by creep when loaded in the range of (0.85-0.95)Q_{ult}^{ref}; and no secondary or tertiary creep was observed below 0.70·Q_{ult}^{ref}. The long-term failure load seems to be 10 to 15% lower than the short-term one. This can be attributed to the rate effects of the natural clay when doing QML tests and to the creep effects described in section 2.3. Torstensson (1973) found that the shear strength obtained from vane shear tests for very low rates (quasi-static drained conditions) was lower than for higher rates, supporting the above results.

In the stepwise loading procedure, each load increment was taken within 2 to 5 minutes (fast loading rate), therefore an undrained response was expected, followed by a transition to drained conditions. Stress states close to the failure envelop triggered high creep rates, that combined with any generated excess pore water pressure from the shearing, lead to failure. Here a combination of long-term accumulated deformations, rate effects, load level and undrained creep behaviour can be the cause for the creep failure.

The creep failure was followed by large displacement of the pile upwards, which in turn

translated into a direct unloading of the pile due to the release of potential energy in the bags. It was observed that the creep rates "stabilized" back when the load reached around $(0.80)Q_{ult}^{ref}$.

Pile 2 is shown In Figure 4.4 as an example of the above results. Each load step is plotted against the logarithm of time. One can see that the slopes of the linear regression curves (i.e. μ^*) increases with the change in load and there is a limit where the pile experiences tertiary creep and fails.

The loads and accumulated displacement for the other piles is given in the Appendix. One can see that the total displacement is different for each pile, been lower for the piles loaded with more steps (more rigid, creep hardening). This hardening effect after creep and relaxation stages has been observed by other researchers (Tian et al., 1994).

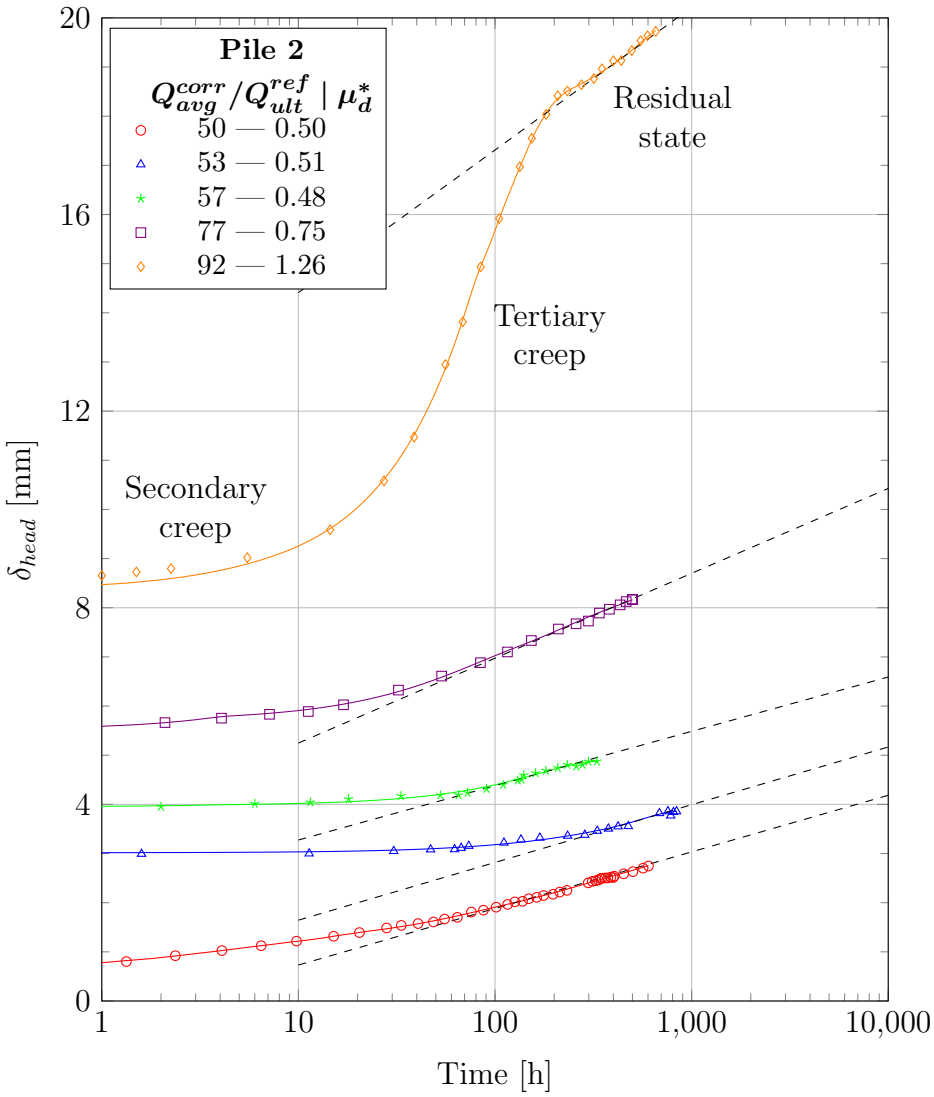

Figure 4.4: *Displacement versus the logarithm of time for each load step. Load ratio and* μ_d^* *parameter in legend.*

4.2.2 Extrapolation

In order to extrapolate the results obtained herein, the logarithmic law in equation 2.4 was used. The creep parameter was determined from the measurement as shown in Figure 4.4. The time was zero set at the beginning of each of load step. The reference time was taken at the bifurcation point between the linear fitted curve and the measurements. This time reference varied with each load step. All creep parameters are presented in Figure 4.5 for all piles with good measurements.

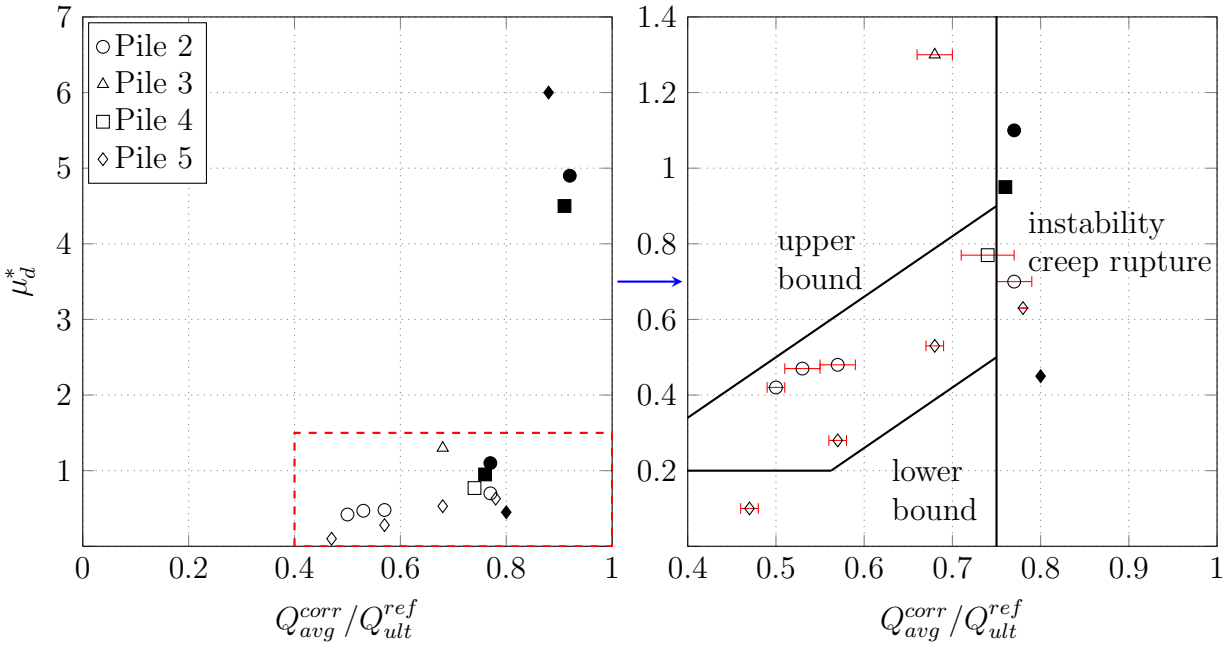

Figure 4.5: *Pseudo creep parameter for the tested piles obtained for each load step with δ_{head} vs $ln(t)$. Solid markers are parameters at creep failure and after failed.*

In order to select a unique reference time, all creep parameters with their respective reference time, were extrapolated to identify the difference in magnitude, see Figure 4.6. Taking 10 days as the unique reference time, the upper bound of 3 mm of displacement was selected as the starting point for the extrapolation of 120 years.

Extrapolation of the creep displacement by using the logarithmic law in equation (2.4) is presented in Figure 4.7. These predictions are for a serviceability life of 120 years. Such types of extrapolations do not take into account effects such as climate change or structuration of the clay. The latter has been observed for very slow strain rates in CRS test and undrained triaxial creep tests, where the clay became stiffer (Augustesen, Liingaard, et al., 2004). Therefore, it does not seem realistic that creep will continue indefinitely since at some point the soil will reach equilibrium for the given stress state (J. Mitchell and Soga, 2005). In general, these results give an idea of the magnitudes to expect in the extrapolated time.

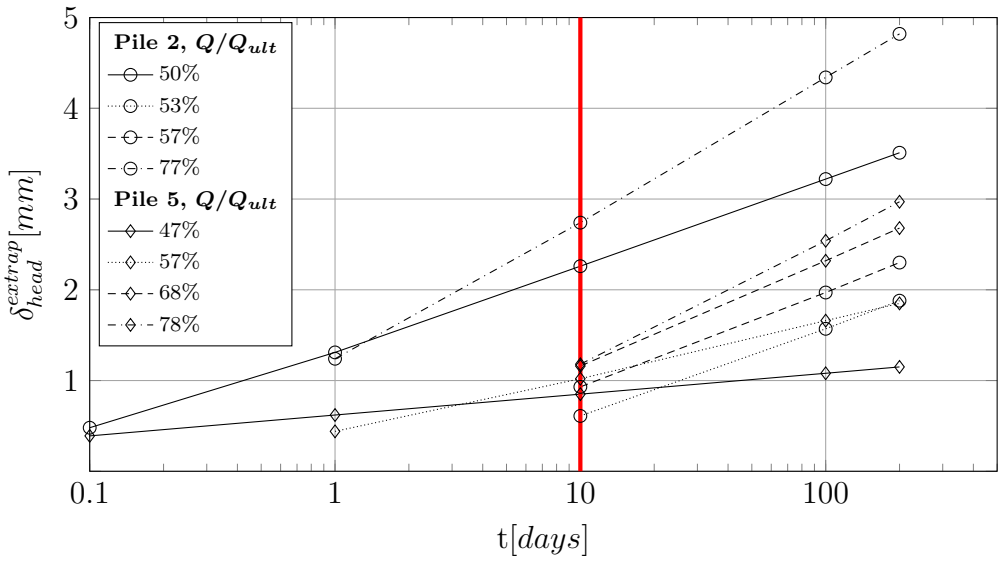

Figure 4.6: *Extrapolation of measurements using the obtained μ_d^* parameters with their respective reference times. All crossing $t = 10$ days.*

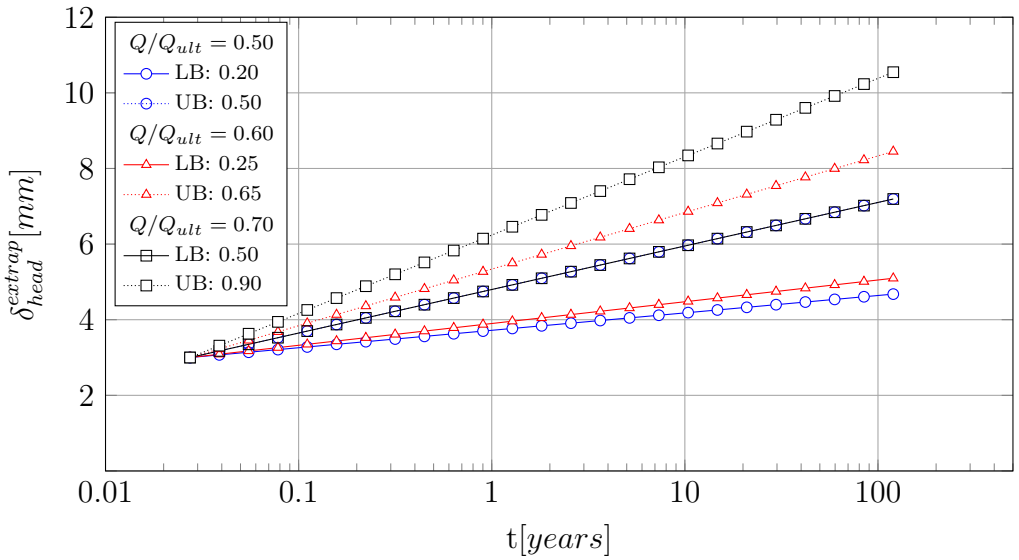

Figure 4.7: *Extrapolation of measurements using the upper and lower bound (UB and LB) of μ_d^* in Figure 4.5 and a unique reference time of 10 days.*

5 Conclusion

The reported field tests generated new experience in pile testing. The novel loading frame provided a simple, yet reliable, method for long-term testing of piles. The results indicate that tension piles, when loaded with design loads used in Swedish practice, exhibit similar behaviour to compression piles in both bearing capacity and deformation. Current ultimate limit state design loads using the α method seem to agree reasonably well with tension loads obtained with the pile load tests commonly used in Sweden.

Due to operational issues in the initial long-term pile tests, the long-term load application was not always "constant" during the whole loading period. Instead it decreased between 5-10% in each load stage. Furthermore, this decay was not with a constant rate, instead it behaved in a cyclic manner (small amplitude and low frequency cycles) following the temperature variations and pile head displacement. These load fluctuations, however, have shown to be insignificant for the long-term pile head displacements, when compared to the results from the highly regulated pile load test.

The magnitude of the long-term displacement measurements have some uncertainty due to (a) tilting of the frame, (b) precise correction for the elastic component from the pulling rod and (c) the stability of the fixed points used to measure the relative displacement of the pile against the soil. Nevertheless, the overall trend of the creep settlement seems to be in good agreement with the tell-tale values, obtained at a larger time interval. The latter were only affected by the stability of the fixed points. Therefore, the magnitude and trend of the tell-tales were considered as the most reliable readings that were subsequently used to correct the other data for the stiffness and temperature effects.

The used extrapolation of the data towards the 120 years estimated has been based on the pile test data. The extrapolated pile head displacement is rather small for both upper and lower bound in case of the $Q/Q_{ult} = 0.60$ load case. Only further analysis of the interface stress and load history in the soil adjacent to the pile will allow to establish the accuracy of the extrapolation method. For now the most important mechanism seems to the possibility of the long-term load triggering creep rupture. One should identify the load limit for this mechanism and design accordingly. Tentatively, the current test data, indicates a limit of 80% of Q_{ult}^{ref} . Although an apparent relation to the short-term creep load determined in the QML tests could be hypothesised this could be coincidental. It is more likely that the long-term failure load is governed by a pure frictional mechanism based on the critical state (or residual state), where any load below the residual strength will not cause creep rupture.

References

Augustesen, A., L. Andersen, and C. S. Sørensen (2006). *Assessment of time functions for piles driven in clay*. Tech. rep. Department of Civil Engineering, Aalborg University.

Augustesen, A., M. Liingaard, and P. V. Lade (2004). Evaluation of time-dependent behavior of soils. *International Journal of Geomechanics* 4.3, 137–156.

Baligh, M. M. (1985). Strain path method. *Journal of Geotechnical Engineering* 111.9, 1108–1136.

Basu, P., M. Prezzi, R. Salgado, and T. Chakraborty (2013). Shaft resistance and setup factors for piles jacked in clay. *Journal of Geotechnical and Geoenvironmental Engineering*.

Bengtsson, P.-E. and G. Sällfors (1983). Floating piles in soft, highly plastic clays. *Canadian Geotechnical Journal* 20.1, 159–168.

Bradshaw, H., R. Barton, and R. McKenzie (1984). "The Hutton TLP Foundation Design". Offshore Technology Conference. DOI: 10.4043/4807-MS.

Campanella, R. G. and Y. P. Vaid (1972). *Creep rupture of a saturated Natural Clay*. Ed. by UBC. Soil Mechanics Series n16. http://webcat1.library.ubc.ca/vwebv/holdingsInfo?bibId=1787450: University of British Columbia.

– (1974). Triaxial and Plane Strain Creep Rupture of an Undisturbed Clay. *Canadian Geotechnical Journal* 11.1, 1–10. DOI: 10.1139/t74-001. eprint: http://dx.doi.org/10.1139/t74-001. URL: http://dx.doi.org/10.1139/t74-001.

Elert, G. (2015). URL: http://physics.info/springs/.

Eriksson, P., L. Jendeby, T. Olsson, and T. Svensson (2004). *Kohesionspålar rapport 100*. Rapport 100. PÅLKOMMISSIONEN.

Fellenius, B. H. (1972). Down-drag on piles in clay due to negative skin friction. *Canadian Geotechnical Journal* 9.4, 323–337.

Fellenius, B. H. (2006). Results from long-term measurement in piles of drag load and downdrag. *Canadian Geotechnical Journal* 43.4, 409–430. DOI: 10.1139/t06-009. eprint: http://dx.doi.org/10.1139/t06-009. URL: http://dx.doi.org/10.1139/t06-009.

Fredrik Klingberg, T. P. and J. Levander (2006). *Bottenförhållanden och geologisk utveckling i Göta älv. Rapport k43*. Tech. rep. Sveriges geologiska undersökning.

Guo, W. (2012). *Theory and Practice of Pile Foundations*. Taylor & Francis. ISBN: 9780415809337. URL: https://books.google.se/books?id=0-XtyVK5c4EC.

Hansbo, S. (1984). "Foundations on friction creep piles in soft clays". *First International Conference on Case Histories in Geotechnical Engineering*.

Hermansson, I., T. Bjerendal, and M. Grävare (2015). *En studie av dynamisk provning jämfört med statisk provbelastning i tryck och drag*. Tekniskt PM 2:2015. PÅLKOMMISSIONEN.

Hultén, A.-M. (1997). *Grundvatten i urban miljö : grundvattnets nivåvariationer i de övre marklagren i Göteborg*. Publ. A - Chalmers tekniska högskola, Geologiska institutionen, no: 85. 61, [36] s. Institutionen för geologi, Chalmers tekniska högskola, ISBN: 992-485149-8.

Jardine, R. and D. Potts (1988). Hutton tension leg platform foundations: prediction of driven pile behaviour. *Geotechnique* 38.2, 231–252.

Jendeby, L. (1986). *Friction piled foundations in soft clay. A study of load transfer and settlements*. Göteborg.

Jostad, H. and J. Yannie (2015). "A procedure for determining long-term creep rates of soft clays by triaxial testing". *International Conference on Creep and Deformation Characteristics in Geomaterials*. 978-91-980974-9-8. Chalmers University of Technology.

Karlsrud, K. (2014). Ultimate Shaft Friction and Load-Displacement Response of Axially Loaded Piles in Clay Based on Instrumented Pile Tests. *Journal of Geotechnical and Geoenvironmental Engineering* 140.12, 04014074. DOI: 10.1061/(ASCE)GT.1943-5606.0001170. eprint: http://dx.doi.org/10.1061/(ASCE)GT.1943-5606.0001170. URL: http://dx.doi.org/10.1061/(ASCE)GT.1943-5606.0001170.

Kullingsjö, A. (2007). "Effects of deep excavations in soft clay on the immediate surroundings". ISBN 978-91-7385-002-5. PhD thesis. Chalmers University of Technology.

Larsson, R. (2007). *Information 15, CPT-sondering: utrustning – utförande – utvärdering*. Tech. rep. SGI, Swedish Geotechnical Institute.

Larsson, R. et al. (2007). *Skjuvhållfasthet - utvärdering i kohesionsjord. Information 3*. Tech. rep. SWEDISH GEOTECHNICAL INSTITUTE.

Lehane, B. and R. Jardine (1994). Displacement-pile behaviour in a soft marine clay. *Canadian Geotechnical Journal* 31.2, 181–191.

Liingaard, M., A. Augustesen, and P. V. Lade (2004). Characterization of models for time-dependent behavior of soils. *International Journal of Geomechanics* 4.3, 157–177.

Mitchell, J. and K. Soga (2005). *Fundamentals of soil behavior*. John Wiley & Sons. ISBN: 9780471463023. URL: https://books.google.se/books?id=b%5C_dRAAAAMAAJ.

Olsson, C. and G. Holm (1993). *Pål Grundläggning*. Ed. by S. geotekniska institut. ISBN 91-7332-663-1. Svensk Byggtjänst, p. 377.

Olsson, M. (2010). *Calculating long-term settlement in soft clays - with special focus on the Gothenburg region*. Lic - Department of Civil and Environmental Engineering, Chalmers University of Technology, no: 2010:3. 115. Institutionen för bygg- och miljöteknik, Geologi och geoteknik, Chalmers tekniska högskola,

– (2013). "On rate-dependency of Gothenburg clay". ISBN 9789173859110. PhD thesis. Chalmers tekniska högskola.

Persson, J. (2004). *The Unloading Modulus of Soft Clay: A field and laboratory study*. Institutionen för bygg- och miljöteknik, Geologi och geoteknik, Chalmers tekniska högskola,

Ramalho Ortigaäo, J. and M. Randolph (1983). Creep effects on tension piles for the design of buoyant offshore structures. *Int Sympo on Offshore Engrg* 12, 16.

Randolph, M. F., J. Carter, and C. Wroth (1979). Driven piles in clay—the effects of installation and subsequent consolidation. *Geotechnique* 29.4, 361–393.

Randolph, M. (2003). Science and empiricism in pile foundation design. *Geotechnique* 53.10, 847–875.

Sagaseta, C., A. Whittle, and M. Santagata (1997). Deformation analysis of shallow penetration in clay. *International journal for numerical and analytical methods in geomechanics* 21.10, 687–719.

Sällfors, G. and L. Andreasson (1985). *Kompressionegenskaper, Geotekniska laboratorieanvisningar, del 10*. Tech. rep. Swedish Geotechnical Society.

Sandegren, E. et al. (1980). *Anvisningar för provpålning med efterföljande provbelastning*. Rapport 59. Pålkommissionen.

SGF, S. G. S. (1993). *Report 2:93E, Recommended Standard for Field Vane Shear Test*. Tech. rep. Swedish Geotechnical Society.

Singh, A. and J. K. Mitchell (1968). General stress-strain-time function for soils. *Journal of the Soil Mechanics and Foundations Division* 94.1, 21–46.

Sivasithamparam, N., M. Karstunen, and P. Bonnier (2015). Modelling creep behaviour of anisotropic soft soils. *Computers and Geotechnics* 69, 46–57. ISSN: 0266-352X. DOI: http://dx.doi.org/10.1016/j.compgeo.2015.04.015. URL: http://www.sciencedirect.com/science/article/pii/S0266352X15000944.

St John, H., M. Randolph, R. McAnoy, and K. Gallagher (1983). Design of piles for tethered platforms. *DESIGN IN OFFSHORE STRUCTURES, 1983,* 61–72.

Tavenas, F., S. Leroueil, P. L. Rochelle, and M. Roy (1978). Creep behaviour of an undisturbed lightly overconsolidated clay. *Canadian Geotechnical Journal* 15.3, 402–423. DOI: 10.1139/t78-037. eprint: http://dx.doi.org/10.1139/t78-037. URL: http://dx.doi.org/10.1139/t78-037.

Tian, W.-M., A. Silva, G. Veyera, and M. Sadd (1994). Drained creep of undisturbed cohesive marine sediments. *Canadian Geotechnical Journal* 31.6, 841–855. DOI: 10.1139/t94-101. eprint: http://dx.doi.org/10.1139/t94-101. URL: http://dx.doi.org/10.1139/t94-101.

Torstensson, B. (1973). "FRICTION PILES DRIVEN IN SOFT CLAY. A FIELD STUDY". PhD thesis. Chalmers Tekniska Högskola.

Trafikverket (2014). *Marieholmsförbindelsen: Markteknisk undersökningsrapport MUR, Geoteknik.* Tech. rep. Trafikverket.

Whittle, A. J. (1987). "A constitutive model for overconsolidated clays with application to the cyclic loading of friction piles". PhD thesis. Massachusetts Institute of Technology.

www.mubea.com. *Mubea Disc Springs Manual.*

Part I

Appendix

Data processing and fix

The raw data was sample every 2 minutes for the first 24 hours and after that every 10 or 15 minutes. Each single sample was made from taking the mean average of 50 samples (f=50Hz) that were first smoothed by a moving average filter (window of 20% of sample group size). Then, the complete data set was smoothed from any noise and outliers by using the same type of moving average described above.

Having the data processed, the next step was to correct it from the initial tilting and the additional elastic component from the pulling rod. After this correction, some points were taken along the complete time of the series and these were used to interpolate a continuous function that could approximate the curve, preserving the trend and magnitude. The latter was done using a Shape Language Modelling tool from Matlab.

Soil characterization

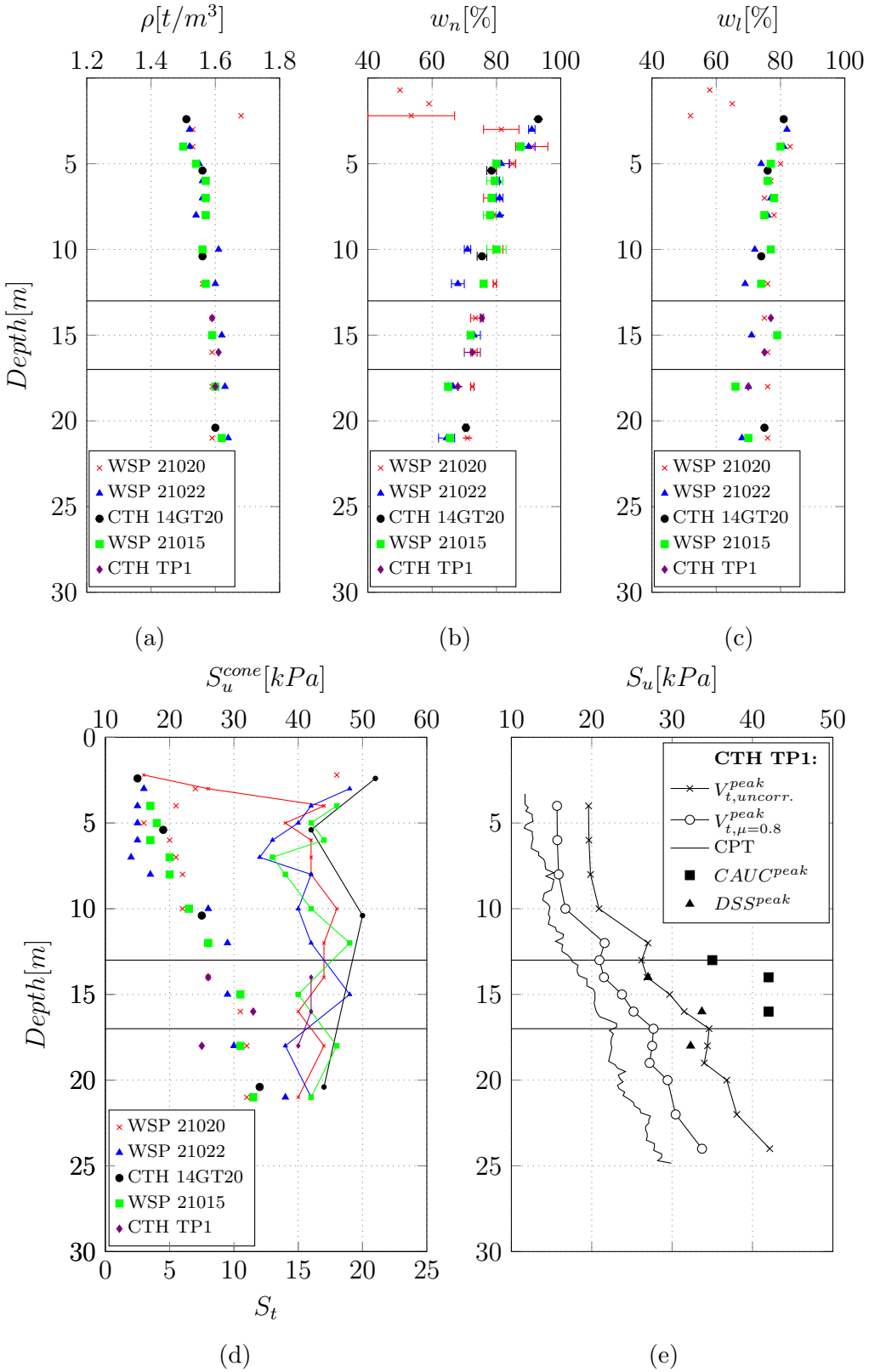

Figure 5.1: *Previous test nearby the area and new tests at the testing site.*

Long-term measurements

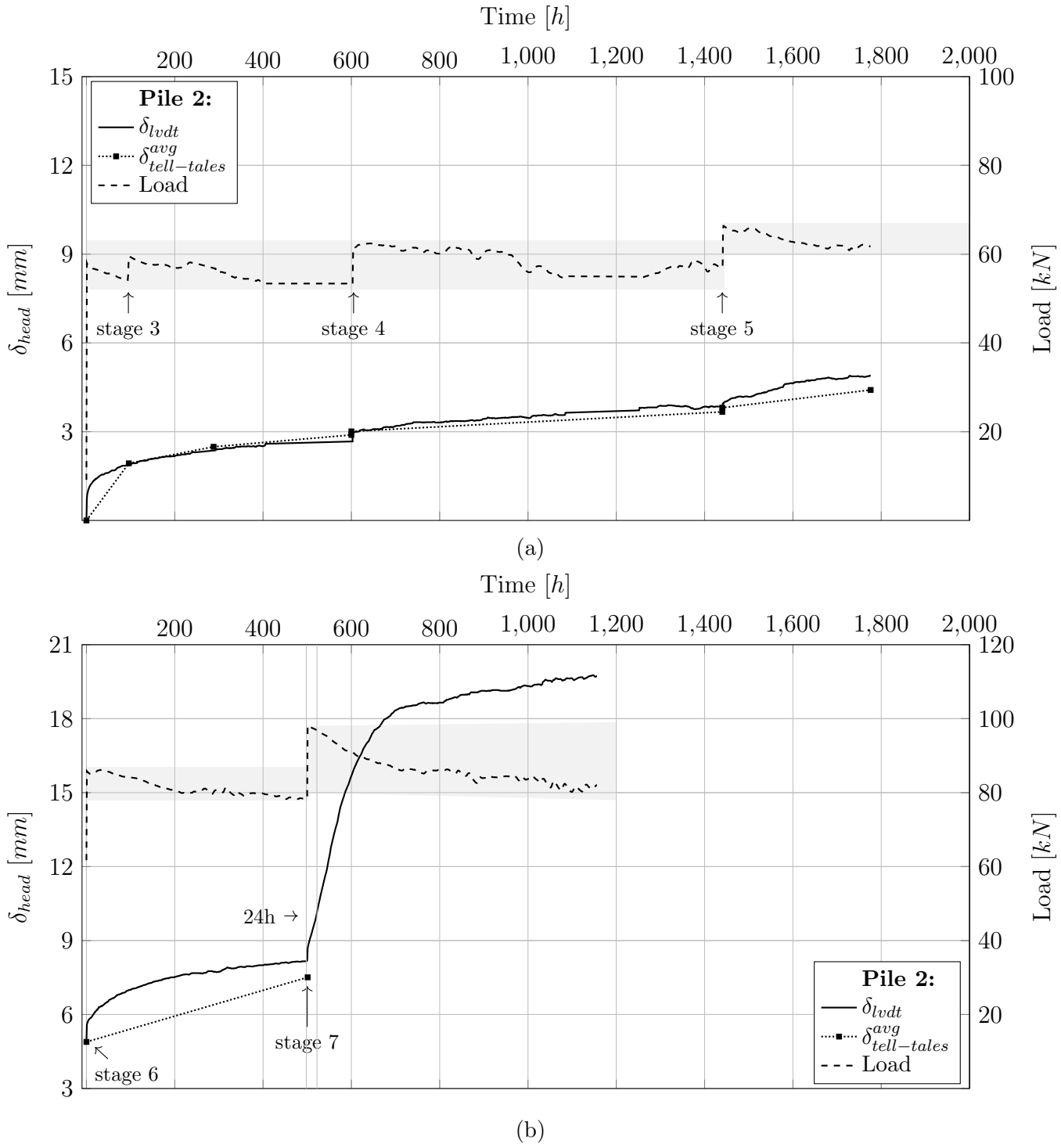

Figure 5.2: *Pile 2. Raw displacement data calibrated against the tell-tale measurements.*

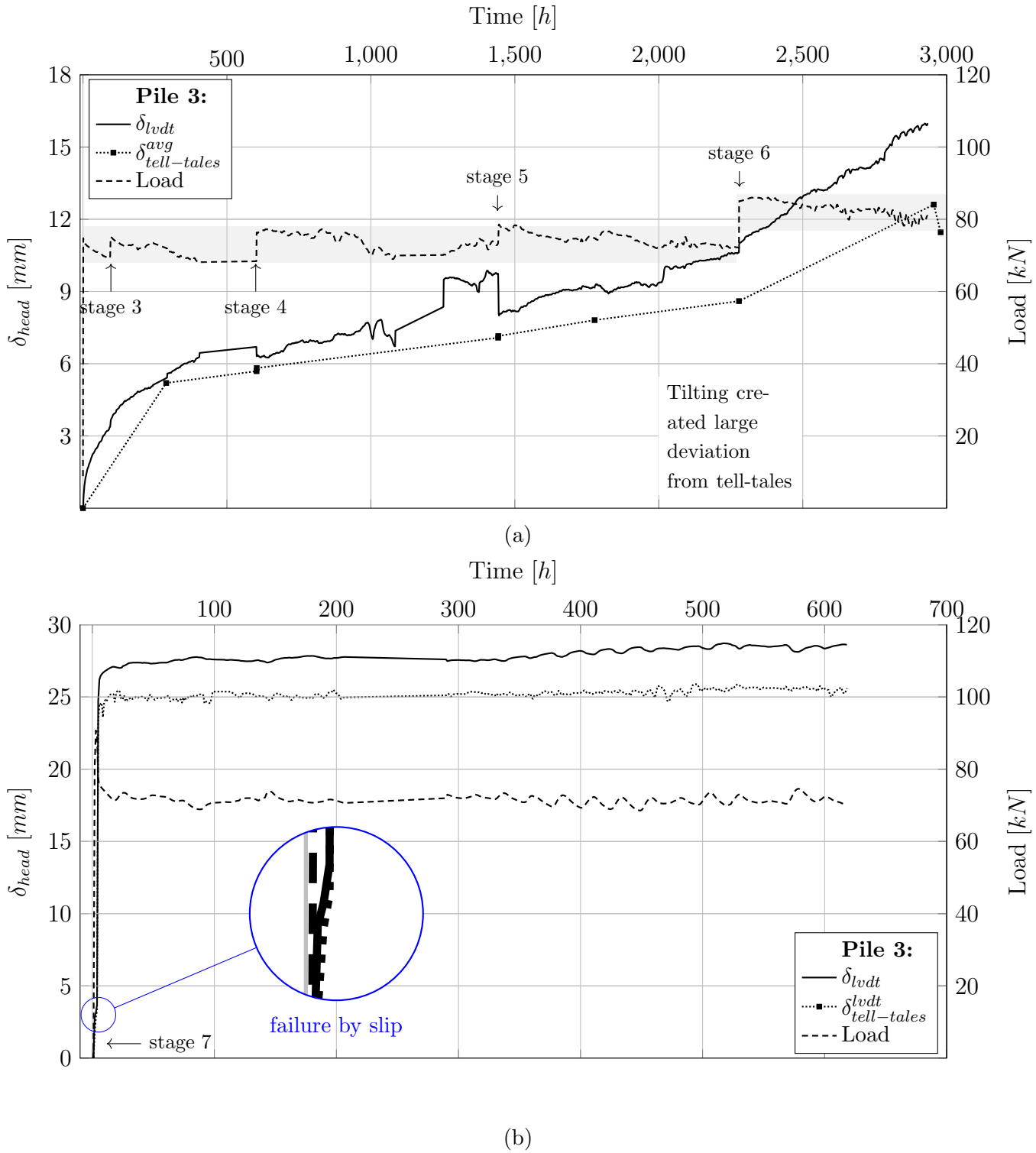

Figure 5.3: *Pile 3. Raw displacement data calibrated against the tell-tale measurements.*

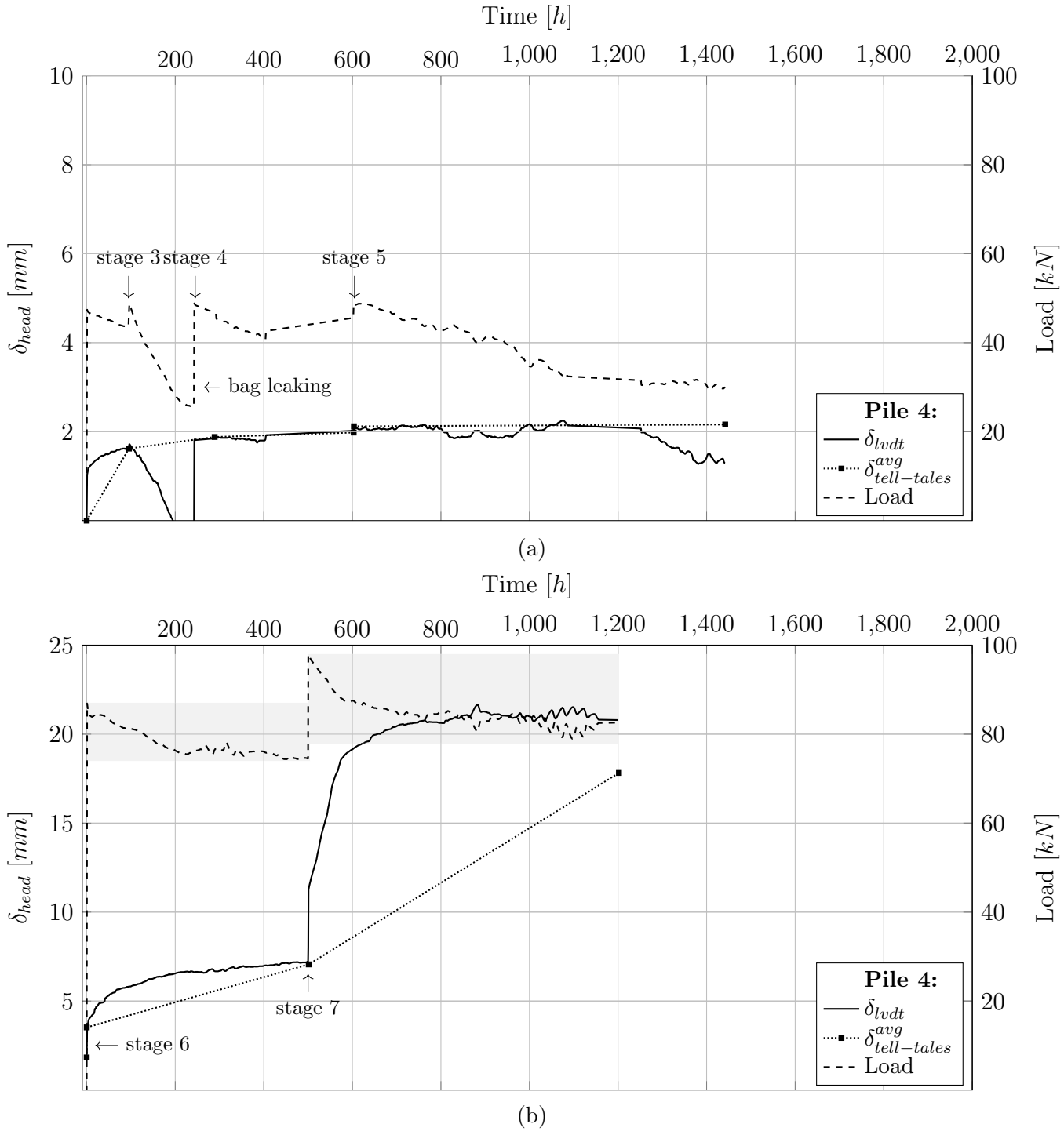

Figure 5.4: *Pile 4. Raw displacement data calibrated against the tell-tale measurements.*

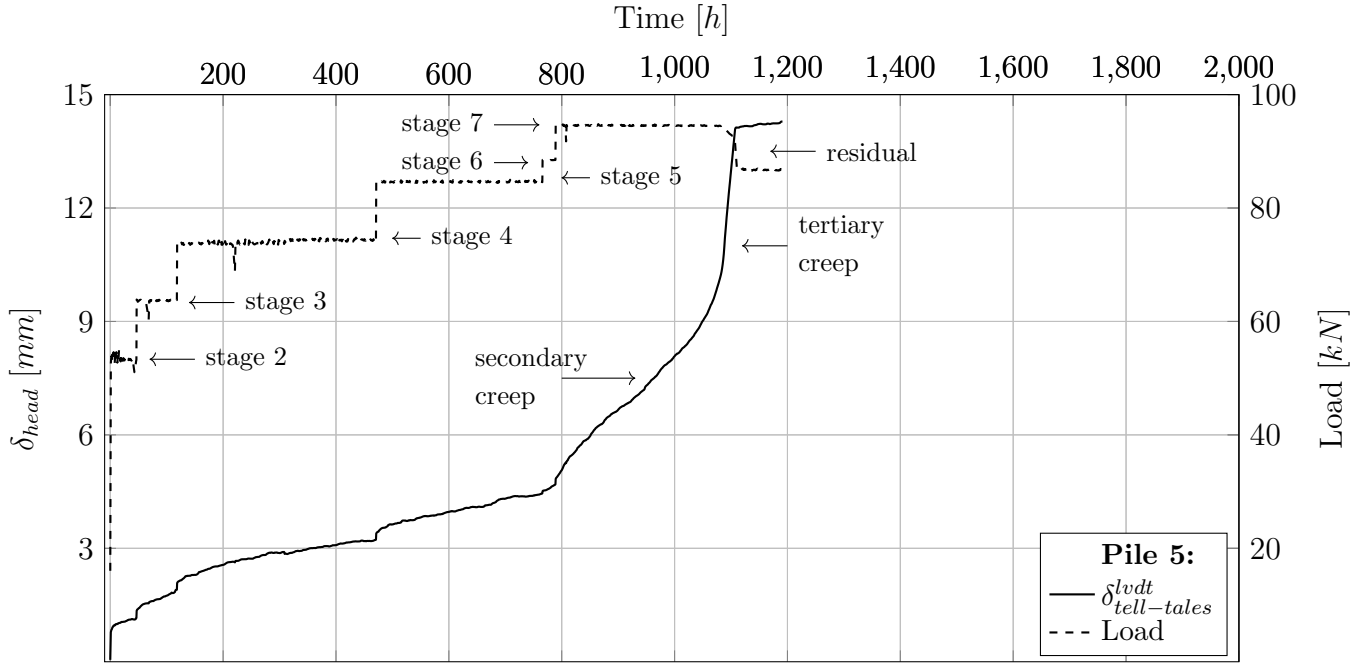

Figure 5.5: *Pile 5. Constant load and LVDTs at tell-tales. Pre-failed in short-term.*